

1 **CENTRAL COMPOSITE DESIGN OF BIODIESEL**
2 **PRODUCTION FROM WASTE COOKING OIL USING**
3 ***TYMPANOTONUS FUSCATUS (PERIWINKLE)***
4 **SHELLS AS CATALYST**
5

6 **ABSTRACT**

Biodiesel has been generally accepted as the environmentally – safer alternative to fossil based fuels. However, concerns of the cost of production, use of acid catalysts leading to corrosion, and recovery of homogenous catalyst remain. This study therefore seeks to optimize the transesterification process parameters in the conversion of waste cooking oil (WCO) using waste *Tympanotonus fuscatus* shell (WFTS). The catalysts were characterized using XRD, FTIR, and XRF. Temperatures ranging from 30°C to 90°C, catalyst loading ranging from 1 to 10% by weight, and reaction durations ranging from 30 to 180 minutes were examined for the transesterification technique. The physiochemical properties of the waste cooking oil revealed a high acid value (10.02mgKOH/g), kinematic viscosity of 13.30 mm²/s, pour point, 156 °C, flash point of 104 °C, Calorific value of 34.78 MJ/kg, carbon content of 2.65 % m/m, among other parameters while the GCMS analysis indicated the presence of C₁₆ to C₂₁. The biodiesel however showed an acid value of 0.416 mgKOH/g, viscosity of 4.638 mm²/s, pour point of 0.3 °C, flash point of 104 °C, calorific value of 40.17 MJ/kg, and carbon content of 0.019 % m/m which were in agreement with the EU and American standards. The elemental composition and crystalline structure of the catalyst revealed a considerable concentration of CaO, MgO, Al₂O₃, SiO₂, and other metal oxides. The CCD approach used to design the experiments was significant (p <0.0001) and the biodiesel synthesis resulted in a maximum yield of 91.70 % was obtained with 5.5 % WFTS, 105 minutes of reaction time, 65 °C, and a 1:7 oil–Methanol ratio. The operating parameters of Temperature (p <0.0001), catalyst load (p = 0.00713), and time (p = 0.0288) all had significant effects on biodiesel yield; however, temperature had a stronger influence than the other process variables. The ANOVA results showed that the factors were extremely significant while Fit statistics and model comparison revealed a coefficient of determination of 97.66%, with the predicted value of 84.68% and the adjusted value of 95.00%. The biodiesel produced met the biodiesel standards.

7 **Keywords:** *Central Composite Design, Heterogeneous Catalysts, Optimization, Response surface*
8 *method, Waste cooking oil, Waste Tympanotonus fuscatus shell (WFTS).*

9 Highlights

- 10 • The waste cooking oil (WCO) was characterized with a high acid value content
11 (10.02 mgKOH/g) and esterified to give an acid value of 0.416 (mgKOH/g).
- 12 • An effective catalyst used for the conversion of waste cooking oil to biodiesel was
13 calcined at 900 °C for 2 hours.
- 14 • The central composite design (CCD) method for optimization was carried out using
15 the three-level, three-factors factorial.
- 16 • Maximum validated biodiesel yield of 91.70 (%wt.) was obtained via numerical
17 optimization.
- 18 • The produced biodiesel quality agrees with biodiesel standard.

19 **1. INTRODUCTION**

20 The depletion of fossil fuel reserves and growing concerns about global warming have not slowed the
21 world's rising energy demand. Conversely, this demand has exacerbated the energy crisis coupled
22 with the growing population and industrial revolution. Renewable energy including solar, wind,
23 geothermal, hydro, and biomass energy sources has become the response to these concerns [1] due
24 to their distinct degradability, economic, and efficient characteristics [2]. Utilizing renewable energy
25 sources is one of the most environmentally friendly ways the energy sector is contributing to
26 sustainable development [3]. Biofuels from biomass has garnered matchless attention among other
27 renewables because of certain disadvantages such as energy storage, influence of seasons on
28 energy generation, unavailability of land mass attributed to other renewables. Contrariwise, the
29 majority of these qualities are innate to biofuels such as biodiesel, biogas, and bioethanol, and can be
30 thought of as defining characteristics of the fuels themselves [2]. Biodiesel stands out among all of
31 these biodegradable fuels as being the one that most closely resembles conventional diesel in terms
32 of its physicochemical properties like low aromatic and sulphur content, high viscosity, low volatility,
33 low calorific value, lubricity, high flash point and cetane content, and overall feedstock regenerability,
34 which can guarantee particulate matter by 47%, hydrocarbon emission by 67% [4], and approximately
35 70–90 % reduction in GHG emission [2], [4]–[9]. These properties make them useful in several
36 automobiles including ships, cars, air planes, amongst others [9].

37 Biodiesel is produced from either the esterification or transesterification reaction (depending on the
38 precursor) of triglycerides including edible and non-edible oils, fat, waste-oils, microalgae gotten from
39 plants and animals [1], [2], [4], [9], [10]. This reaction is carried out in the presence of an alcohol and
40 a suitable catalyst to produce esters and water or fatty acid alkyl esters and glycerol respectively. The
41 use of non-edible oil sources like *Jatropha* oil, neem oil, and rubber seed oil, amongst others, micro
42 algae, and waste cooking oil (WCO) has been considered an appealing option that has the potential
43 to lower the cost of producing biodiesel while ameliorating the concerns of food shortages due to the
44 use of edible oils as biodiesel feedstock [2], [8], [11]–[14]. Millions of tons of WCO are being
45 generated yearly with about 1 million from Malaysia [15], and a total of about 16.5 million tons
46 worldwide [3], [16]–[18]. These volumes which are being wasted by open disposal on plants and
47 animals alike [19] can be collected and converted into biodiesel creating dual-faced solution:
48 prevention of environmental degradation and alternative feedstock for the energy sector [1], [12], [19].

49 In general, catalysts can be categorised as homogenous or heterogeneous. Homogeneous base
50 catalysts exhibit a high level of catalytic activity under mild reaction conditions (40 to 65°C at normal
51 atmospheric pressure) [14], [20]. However, homogeneous catalysts are plagued by technical issues
52 such as soap formation, reactor corrosion, difficult catalyst recovery, and the production of vast
53 quantities of polluted water, which increase the overall cost and dangers of biodiesel production [21]–
54 [23]. Due to their eco-friendly and recyclable catalytic activities, the use of bio-based heterogeneous
55 catalysts in biodiesel production has received special consideration [23], [24]. Heterogeneous
56 catalysis has the potential to mitigate the various difficulties encountered when using homogeneous
57 catalysts to produce biodiesel from low-cost feedstock. Heterogeneous catalysts have a number of
58 technical benefits, including simple separation and purification of reaction products, low production
59 cost, decreased reactor corrosion, high stability, and low sensitivity to free fatty acids and moisture
60 contents [23], [25]. Many research communities are focused on developing novel heterogeneous
61 catalysts that are stable, durable, and efficient under ambient conditions [26]. Several research has
62 focused on the exploitation of waste materials as catalysts (wood [27], sugar cane bagasse and oil

63 palm trunk [28], corn cub [10], fly ash [5], [28], [29], wheat bran [23], egg and coconut shells [25],
64 [30], plantain [31] and banana [32] peels, bones [33], etc.), due to their abundance and low cost of
65 catalysts preparation. Solid base catalysts have higher catalytic activity than solid acid catalysts [34].
66 Different solid-base catalysts used in transesterification include CaO, MgO, Al₂O₃, SiO₂ etc. [35],
67 KF/Al₂O₃. These catalysts produce over 92% yield of biodiesel under optimum reaction conditions.

68 A large portion of Nigeria's 12 million tonnes of waste shells are *Tympanotonus fuscatus* (Periwinkle)
69 shells [36]. After consuming the edible part, the shells become waste and litter trash dumps,
70 residential areas, and even local markets, causing land and air pollution [37]. Decomposing waste
71 shells produce an offensive stench, leach and weather heavy metals from the dump, and contaminate
72 public water systems [36], [38]. Several shells from eggs [5]–[7], [11], [25], [28], [39]–[41] and a
73 variety of snails [40], [42]–[48] have been used, however, there aren't many studies [22], [49], [50] in
74 literature on the use of WTFS as a heterogeneous catalyst for biodiesel production.

75 In this research, the bio-catalytic (WTFS) synthesis of waste cooking oil (WCO) was investigated
76 through a two-step esterification and transesterification reaction. The synthesized catalyst was
77 characterized by XRD, XRF, and FT-IR for functional groups, elemental composition, and crystalline
78 structure. The WCO was pre-treated and stored for consequent characterization. Optimized Trans-
79 esterification reaction was then carried out using the central composite design (CCD) of experiments
80 and the products obtained were subsequently characterized for their physicochemical properties,
81 alongside their functional groups (FT-IR), and GC-MS to determine the effect of the catalyst on the
82 WCO. The catalyst was synthesized as recommended for the great performance breakdown of
83 hydrocarbon chains. The central composite design (CCD) is a tool for statistical optimization that is
84 used to maximise the many different factors that are involved in the system. CCD is the optimization
85 method that is advised to use CCD is recommended when there are more than two factors at play in
86 the system and the optimal value lies in the middle of the factor ranges. To optimise the biodiesel
87 synthesis process, reaction parameters such as WTFS catalyst loading (wt. percent), reaction
88 temperature (°C), and residence time (minutes), were considered while the Response Surface
89 Methodology (RSM) of statistical optimization technique based on CCD was utilised.

90 This work is original for several reasons:

- 91 i) Designed and characterized a functional heterogeneous catalyst for biodiesel production from an
- 92 agricultural waste i.e. *Tympanotonus fuscatus* shell, which is abundant in the entire Southern-Nigeria;
- 93 ii) Optimized catalyst preparation parameters including activation with sulphuric acid, temperature and
- 94 duration;
- 95 iii) Adoption of WTFS catalyst to produce biodiesel from high free fatty acids waste cooking oil;
- 96 iv) Optimization of the biodiesel production conditions with a full factorial design of experiments in
- 97 conjunction with response surface methodology via central composite design;

98 The optimally produced biodiesel was characterised in accordance with ASTM and European
99 (EN14214) standards. The most important aspect of this research is unquestionably the investigation
100 into the synthesis of a bio-based heterogeneous catalyst.

101 **2. EXPERIMENTAL**

102 In the following is a list, functionality, and description of the materials and methods used to carry out
103 the preparation, characterization, and experiment.

104 **2.1 Materials**

105 **2.1.1 WCO and WTFS**

106 The waste cooking oil (WCO) was provided by a local restaurant (chicken republic) in Ugbowo area of
107 Benin city, while the WTFS was collected from Uselu Market, all in Benin city area of Edo State,
108 Nigeria. The WCO collected is filtered, to remove any impurity and suspended matter or particles.
109 **This was heated at 120 °C** while stirred continuously for 2 hours to remove possible water content.
110 The pre-treated WCO was hereafter stored in a clean container. The WTFS collected was thoroughly
111 washed with water for three days consecutively to remove the dirt and remnant periwinkle flesh within
112 the shells. The WTFS was then dried in direct sunlight for 3days to reduce the foul smell.

113 **2.1.2 Chemicals**

114 Distilled water, 99.5% pure methanol, Concentrated Sulphuric acid (H₂SO₄), Ethanol, Benzene,
115 Potassium Hydroxide (KOH), Hydrochloric acid (HCl), Acetic acid, Chloroform, Wijs reagent,
116 Phenolphthalein, Sodium thiosulphate, Potassium Iodide (KI), starch solution indicator, ice block.
117 They were all of analytical grade obtained from Ken Chemical Shop, Benin city, Nigeria, and needed
118 no further purification.

119 **2.2 Methods**

120 **2.2.1 Preparation of Catalyst**

121 The preliminary sun-dried WTFS was further dried in oven (U-Tech SSI-107) at an average of 120 °C
122 for 24 hours to remove excess water [51] before calcining in the electric-powered furnace
123 (MXBAOHENG YTH-2.5-10) at a temperature rate of 0.1 °C/second till 900 °C [52] and then left for an
124 additional 2 hours to ensure complete oxidation and convert any carbonate to oxides and bring out
125 the maximum amount of metallic oxides. The calcined WTFS was then cooled before subjecting to
126 pulverization manually with the use of a mortar and pestle to obtain fine powder. This was repeated
127 three (3) times with the use of a sieve of mesh size 45µm to ensure proper separation, homogeneity,
128 and diffraction of powdered catalyst. To avoid the use of contaminated active oxides in the WTFS
129 catalyst from exposure to atmospheric water, moisture and carbon dioxide thereby forming less active
130 hydrates and inactive carbonates, the powdered WTFS was then re-calcined again at 900 °C for 1
131 hour before removal from furnace and storage in a sealed glass desiccator while the temperature
132 dropped to room temperature.

133 **2.2.2 Characterization of Catalyst**

134 The X-ray diffraction (XRD) of the WTFS derived catalyst was performed on a sample of WTFS using
135 the Brucker's D2-PHASER benchtop X-ray powder diffractometer furnished with Cu-Kα (1.541874 Å)
136 radiation source. The XR software was set to 40KV and 40mA while the scan interval was from 10°
137 to 90° 2θ with a step size of 0.02. The XR patterns of Ca, Mg, Al and Si majorly amongst others were
138 collected at the 2θ axis of the detector using the powder method in a scintillating diffractometer.

139 The elemental chemical compositions of the materials were analysed using the HORIBA's MESA-50K
140 X-ray fluorescence spectroscopy (XRF) to determine the compounds present (CaO, MgO, Al₂O₃ and
141 SiO₂). The functional groups were determined by Fourier transform infrared (FT-IR, Bio-Rad 3000
142 Excalibur series with wave number range from 400 to 3000 cm⁻¹).

143 **2.2.3 Characterization of WCO and Biodiesel**

144 The characteristics of the WCO, and Biodiesel was determined by relevant techniques based on
145 majorly on ASTM and European (EN14214) International standards. The relative density was
146 determined using ASTM D4052, the Kinematic viscosity was determined using the ASTM D7042. The
147 Acid Value was determined using the ASTM D974 testing standards, Peroxide value was determined
148 as described by the ASTM D3703 method, ASTM-D1959-97 was used to determine the Iodine value,
149 ASTM D94 was used for the saponification value. The Glycerol content, Ester value and Free Fatty
150 Acid (FFA) were both gotten from the saponification value and acid vales respectively. Pour point was
151 determined using the American Standards for Testing and Methods in ASTM-D97, Pensky-Martens
152 equipment was used to determine the flashpoint (ASTM-D93), ASTM-D2500 for cloud point, ASTM-
153 D4297 for calorific value, and ASTM-D1500 standards was used to determine the carbon content.

154 Gas Chromatography coupled with Mass Spectrophotometry (GC-MS) of Hewlett-Packard HP 7890
155 was used to analyse the chemical composition of produced biodiesel. 5% phenylmethypolysiloxane
156 was used to form a thick-film coating on the capillary column working with a 5975-quadrupole
157 detector. The temperature ranged from 50 °C to 290 °C at the rate of 5 °C per min for 10 min in full
158 scan mode between m/z 33-533 using split-less injection function at 290°C and solvent interval of 3
159 min. The obtained peaks based on their retention times were matched with standard compound peaks
160 of NIST08s mass spectral data library.

161 **2.3 Biodiesel production**

162 **2.3.1 Esterification Reaction**

163 The transesterification of WCO was initially carried out with a 7:1 methanol – oil ratio, temperature of
 164 60 °C, 5.5 % WTFS catalyst loading for 180 °C [53]. This yielded 21.35% biodiesel with plenty of soap
 165 formation along with the large amount of water proving Canakci & Sanli [54] right. Hence, since the
 166 conversion of oil to biodiesel can only be carried out with FFA of less than 1% [55], it became
 167 necessary to first esterify the oil (500 g) with sulphuric acid (5 g) dissolved in methanol (24 g) for
 168 1hour at 60oC [53], [55]. Canakci [54] & Thangaraj [55] posited that the most common way is to
 169 convert free fatty acids into FAME by esterification using sulphuric acids, p-toluene sulfonic acids, or
 170 alkyl benzene sulfonic acids.

171 The mixture was heated in a three-neck round bottom flask connected with a reflux condenser to
 172 avoid methanol losses and heated on a magnetic stirrer with a thermocouple installed to keep the
 173 temperature constant. After completion of the reaction, the mixture was poured in a separation funnel
 174 and left to cool and settle overnight into two layers. Water in the lower layer was removed while FAME
 175 and unreacted triglyceride was subjected to the other transesterification process. This esterification
 176 process reduced the FFA content from 5.03% to 1.02% before transesterification with WTFS catalyst
 177 was carried out.

178 2.3.2 Synthesis of Biodiesel

179 The transesterification reaction made use of a recommended 7:1 methanol – oil ratio, while three
 180 factors were varied; temperature ranging from 30 °C to 90 °C, WTFS catalyst loading of 1 to 10 %wt.
 181 and residence time ranging from 30minutes to 180minutes [53], [56]–[61]. The process began with
 182 weighing a known amount of the pre-treated oil and heating in a three-necked batch reactor to its
 183 specified reaction temperature according to the central composite experimental design (CCD). The
 184 catalyst is the weighed and dissolved in methanol with its ration to oil being set to 7:1 constant as the
 185 minimum optimal ratio needed to achieve over 80% conversion [53]. At the end of the reaction, the
 186 reaction mixture was then transferred into the separation funnel and left overnight to allow the
 187 separation of catalyst, glycerol and biodiesel (in that order from bottom to top). The upper phase
 188 (biodiesel phase) was obtained and further purified using a high-speed centrifuge to remove any
 189 suspended catalyst or glycerol. The purified biodiesel was stored in a closed-tight vial to be used for
 190 biodiesel characterization using Agilent Technologies 7890B GC system –5977A MSD (GC-MS) and
 191 Perkin Elmer Spectrum TM 100 FT-IR spectroscopy. The conversion was calculated in percentage
 192 using Equation (1).

$$193 \text{ Biodiesel Yield (\%)} = \frac{\text{Weight of Biodiesel}}{\text{Weight of WCO}} \times 100\% \quad (1)$$

193 2.3.3 Design of experiment for biodiesel production, ANOVA statistics, and 194 optimization

195 Three factors were studied; the amount (in weight percent) of WTFS (1 – 10 %wt. in relation to the
 196 acid), reaction temperature (30 °C – 90 °C) and reaction time (30 – 180 minutes). RSM was employed
 197 to analyse the operating conditions of the transesterification reaction to obtain a high conversion
 198 percent. The experimental design was carried out by the three chosen independent process variables
 199 at three levels. The software “Design Expert 8P” was used for designing and analysing the
 200 experimental data. The independent variables (factors) and their levels, real values as well as coded
 201 values are presented in Table 1 below generating twenty (20) experimental runs all together.

202 **Table 1**
 203 Experimental design for transesterification of WCO

Name	Unit	Low	High	- alpha	+ alpha
Temperature	oC	42.16	77.84	30	90
Catalyst load	wt. %	2.82	8.18	1	10
Time	minutes	60.40	149.60	30	180

204

205 The model equation was used to predict the optimum values and subsequently to elucidate the
 206 interaction between the factors. The quadratic equation model for predicting the optimal point was
 207 expressed according to Equations (1) below and the response (y) was determined to be the biodiesel
 208 yield [62].

$$y = \beta_0 + \sum_{i=1}^k \beta_i x_i + \sum_{i=1}^k \beta_{ii} x_i^2 + \sum_{i=1}^{k-1} \sum_{j=i+1}^k \beta_{ij} x_i x_j + \varepsilon \quad (2)$$

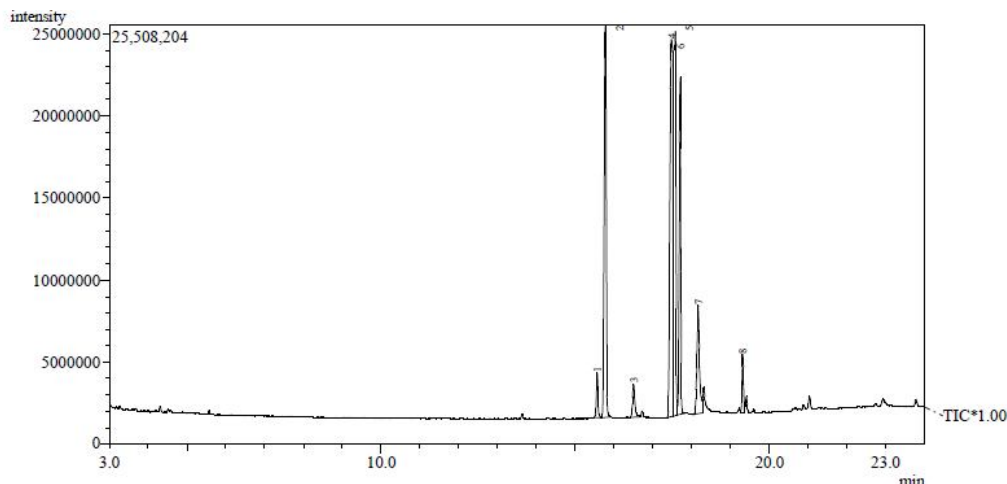
209 The analysis of variance (ANOVA), was the statistical tool used for analysis used to establish the
 210 influence of each variable on the response (biodiesel) yield. The statistical analysis further produced
 211 the predicted values which were compared and contrasted with the responses obtained. On the
 212 output-factors graph, the anticipated value was plotted against the responses to reveal the lines-of-
 213 best-fit, which demonstrated the relationship between the considered variables. The process was
 214 optimized by determining the and sum of squares and lack of fit test. Specifically, the df, f-value, p-
 215 value, coefficient of determination (R-square), and regression co-efficient (experimented and
 216 predicted R-square values) were examined to demonstrate the suitability of the model. Graphing a
 217 function with a multi-dimensional input (AB; AC; BC; ABC) and a one-dimensional output (biodiesel
 218 yield) necessitates the charting of points in three-dimensional space to examine the effect of
 219 interaction variables.

220 3. RESULTS AND DISCUSSION

221 3.1 Properties of WCO, Biodiesel

222 The GC-MS results (Figure 1) for the characterization of WCO are outlined in Table 2 below. For
 223 comparison purposes, they are tabled together with the Biodiesel results (Table 5). WCO trans-
 224 esterified in the presence of WTFS produced biodiesel which fell within the biodiesel European
 225 standard (EN 14214:2003) as shown in Table 2 below. Also, comparing the properties with the
 226 petroleum diesel is necessary for determining the validity of the biodiesel.

227



228
229

Figure 1 GCMS Spectra of WCO showing peaks at different time intervals

230
231
232
233

Table 2
Fatty Acid Profile of WCO

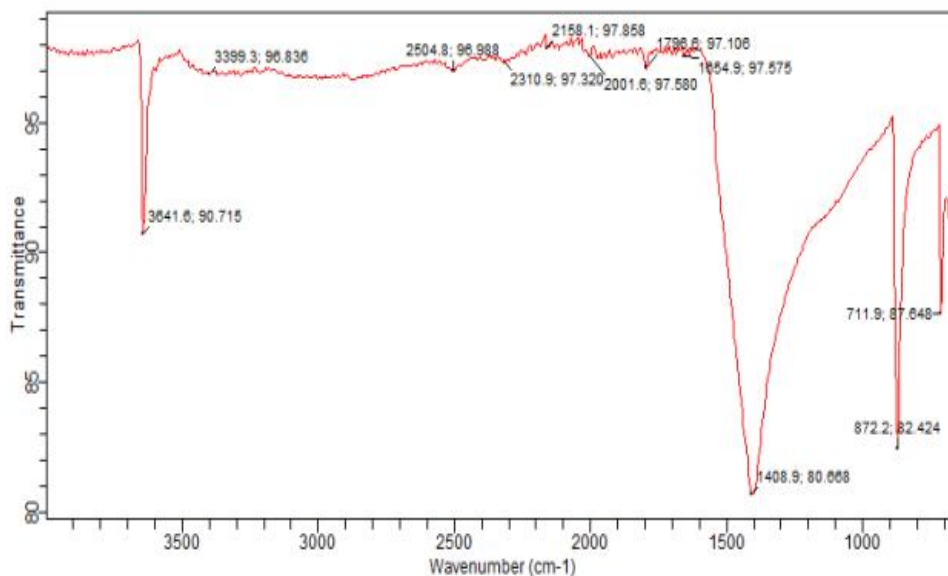
Peaks	R Time	Compound	Area (%)
1	15.570	C19H36O2 Methyl (11E)-11-octadecenoic acid	1.67
2	15.790	C17H34O2 Methyl 14-methylpentadecanoic acid	21.50
3	16.511	C16H32O2 1-Pentadecanecarboxylic acid	1.91
4	17.486	C18H31ClO (9E,12E)-9,12-Octadecadienoyl chloride	26.43

5	17.583	C ₁₉ H ₃₆ O ₂ (E)-9-Octadecenoic acid methyl ester	26.20
6	17.710	C ₂₁ H ₄₂ O ₂ Methyl-aracidate or Methyl-eicosenate	12.92
7	18.176	C ₁₈ H ₃₄ O ₂ cis-9-Octadecenoic acid	7.20
8	19.320	C ₁₉ H ₃₆ O ₃ Methyl ricinolate	2.26

234

235

3.2 WTFS Characterization and Elemental Analysis



236

237

Figure 2 FT-IR spectra of the WTFS catalyst

238 Figure 2 shows the FT-IR spectra analysis of the WTFS catalyst calcined at 900 °C for 2 hours after
 239 pre-treatment. The absorbance bands match the WTFS vibrations during infra-red exposure. Table 3
 240 gives the functional groups in the WTFS catalyst according to the spectrum stretching.

241 **Table 3**

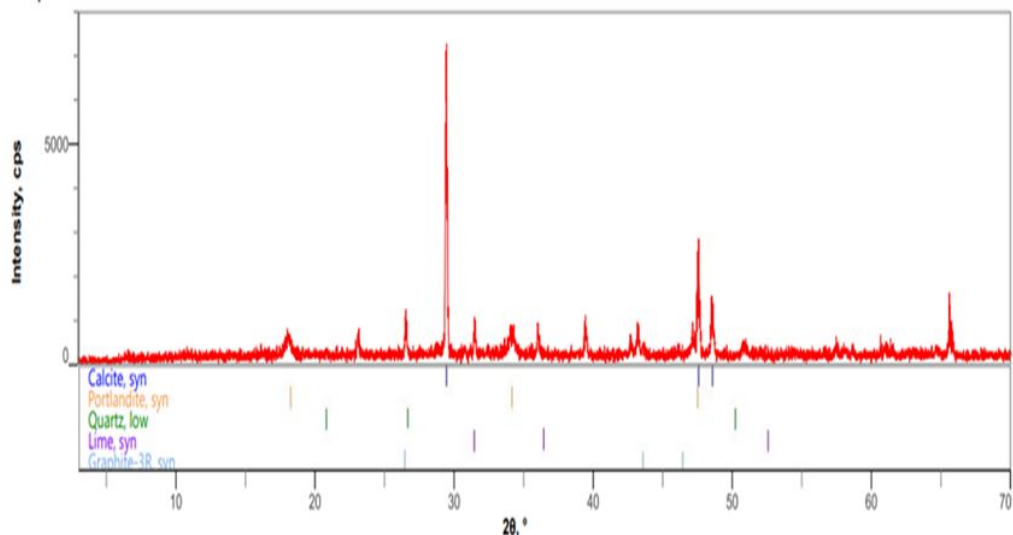
242 Functional groups of WTFS catalyst

S/No.	Frequency (cm ⁻¹)	Appearance	Bonds	Compounds
1.	3641.6	Very sharp and weak absorption band	O-H stretching vibration (free)	Alcohols, phenol, water, ROH, ArOH, H ₂ O
2.	1408.9	Very sharp and broad absorption band	C-O stretching vibration of carbonate ion	CO ₃ ⁻ , CO ₂ , CO
3.	872.2	Very sharp and broad absorption band	C-H bending vibration	RCH=CR, or mono substituted Arene ring
4.	711.9	Very sharp and broad absorption band	M-O stretching vibration	Ca – O, Mg – O, Al – O etc.

243

244 The XRD pattern of WTFS catalyst reflects the properties of a crystalline material with a single intense
 245 and sharp basal plane peak at low 2θ, a medium duplet, and a basal plane peak at high 2θ. All of the

246 reflections are crisp, indicating that the material is extremely crystalline and contains few impurities.
 247 The XRF analysis gives the elemental composition confirmed by the XRD in Figure 3. It shows a high
 248 concentration of CaO of 57.104 wt%, MgO of 21.195 wt%, Al₂O₃ of 13.949 wt%. This shows that the
 249 WTFS catalysts is comprised mainly of CaO, MgO and Al₂O₃. The other metal oxides present in the
 250 catalyst include PdO of 4.203 wt% while others are very low and has insignificant effect on the
 251 properties of the catalyst. These transition metals and their compounds are used as catalyst because
 252 of their ability to change oxidation state or in the case of the metals, to adsorb other substances on
 253 their surface as catalyst.



254
 255 **Figure 3** X-ray diffraction of WTFS catalyst

256 **3.3 Transesterification reaction of WCO**

257 **3.3.1 Numerical optimization of reaction conditions for WCO to biodiesel using WTFS**

258 **Table 4** RSM experimental design matrix and results of produced biodiesel.

Standard order	Coded factors			Actual factors			Yield (%)	
	A	B	C	Temp (°C)	Catalyst dosage (wt.%)	Time (mins)	Experimental	Predicted
1	-1	-1	-1	42.16	2.82	60.40	77.56	79.75
2	1	-1	-1	77.84	2.82	60.40	65.12	63.19
3	-1	1	-1	42.16	8.18	60.40	57.47	52.73
4	1	1	-1	77.84	8.18	60.40	22.70	26.02
5	-1	-1	1	42.16	2.82	0	58.22	53.10
6	1	-1	1	77.84	2.82	0	40.18	43.12
7	-1	1	1	42.16	8.18	0	83.96	82.61
8	1	1	1	77.84	8.18	0	67.93	63.94
9	1.68	0	0	30.00	5.50	0	48.84	52.46
10	1.68	0	0	90.00	5.50	0	22.67	21.60
11	0	-1.68	0	60.00	1.00	0	71.90	72.17
12	0	1.68	0	60.00	10.00	0	64.68	66.96
13	0	0	-	60.00	5.50	30.00	67.75	67.57

			1.68						
14	0	0	1.68	60.00	5.50	180.0	0	74.34	77.06
15	0	0	0	60.00	5.50	105.0	0	81.75	84.09
16	0	0	0	60.00	5.50	105.0	0	80.16	84.09
17	0	0	0	60.00	5.50	105.0	0	82.18	84.09
18	0	0	0	60.00	5.50	105.0	0	85.81	84.09
19	0	0	0	60.00	5.50	105.0	0	79.23	84.09
20	0	0	0	60.00	5.50	105.0	0	86.95	84.09

259

260

261

262

263

264

265

266

267

268

269

The numerical optimization of the transesterification of WCO was carried out with the use of design expert software 8P using response surface methodology. Central Composite Design (CCD) was recommended by the software based on the three-factors, three-level design. The quadratic model was chosen, the build time was 10 minutes and the subtype, randomized to generate 20 runs as presented in Table 4. From the table, the highest biodiesel yield was 86.95% at the following conditions; 60 °C temperature, 5.50 wt. % catalyst loading, 105 minutes, and a constant methanol – oil ratio of 7:1. These results were analyzed numerically and Table 5 was gotten:

Table 5

ANOVA results for the quadratic response surface regression model

Source	Sum of Squares	Df	Mean Square	F-Value	p-value Prob > F
Model	6966.331	9	774.0368	46.33446	< 0.0001*
A-Temperature	1149.475	1	1149.475	68.8085	< 0.0001*
B-Catalyst Load	3279.335	1	3279.335	9.63033	0.00713*
C-Time	108.665	1	108.665	6.504776	0.0288*
AB	51.6128	1	51.6128	3.089583	0.1093
AC	21.58245	1	21.58245	1.291943	0.2822
BC	1682	1	1682	100.6859	< 0.0001*
A ²	3742.421	1	3742.421	224.0243	< 0.0001*
B ²	306.5278	1	306.5278	18.349	0.0016
C ²	190.7235	1	190.7235	11.41686	0.0070
Residual	167.0542	10	16.70542		
Lack of Fit	119.6566	5	23.93133	2.52453	0.1662
Pure Error	47.3976	5	9.47952		
Cor Total	7133.385	19			

Fit Statistics	
R ² (%)	97.66
Adjusted R ² (%)	95.00
Predicted R ² (%)	84.68
Coefficient of Variation	06.20
Adequate Precision	21.00

270

271

272

273

274

275

276

277

* means significant factors

The Model F-value of 46.33 implies the model is significant. This means that there is only a 0.01% chance that a "Model F-Value" this large could occur due to noise. Based on the analysis of variance (ANOVA), the "p-value" value determined for the quadratic model was less than 0.05, suggesting that the design factors was significant. This means that the temperature (Factor A; p-value is < 0.0001), catalyst load (Factor B; p-value is 0.00713), time (factor C; p-value is 0.0288) and various interactions like;

278

- Interactions between the catalyst load and time (factor BC; p-value is < 0.0001)

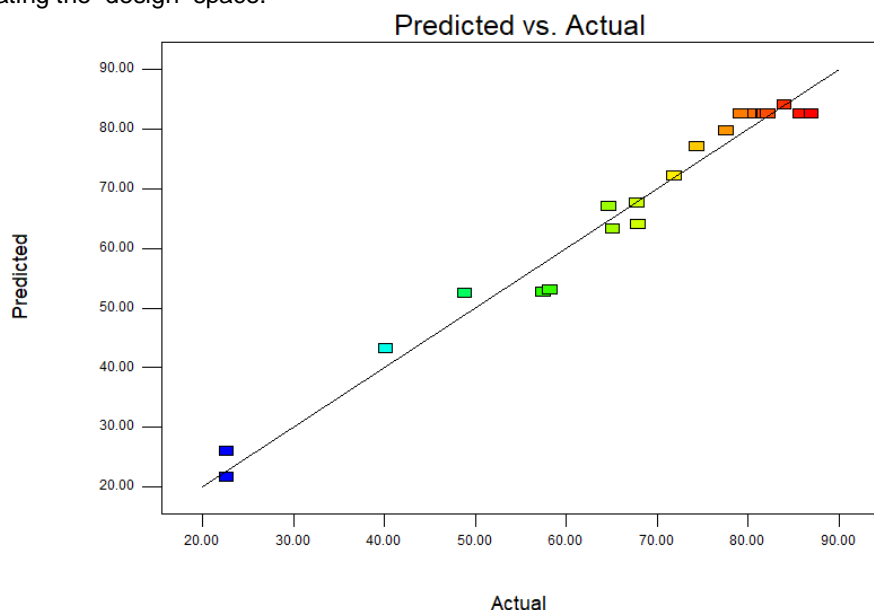
279 • Quadratic factors; square of the temperatures (Factor A²; p-value is < 0.0001), catalyst load
 280 squared (Factor B²; p-value is 0.0016) and time squared (Factor C²; p-value is 0.007).

281 Furthermore, to demonstrate the connection between biodiesel yield and the three significant factors,
 282 the interaction and the quadratic factors, the quadratic equation for the regression model in Equation
 283 (3) below is used:

$$Yield = 82.61 - 9.17A - 1.55B + 2.82C - 2.54AB + 1.64AC + 14.50BC - 16.11A^2 - 4.61B^2 - 3.64C^2 \quad (3)$$

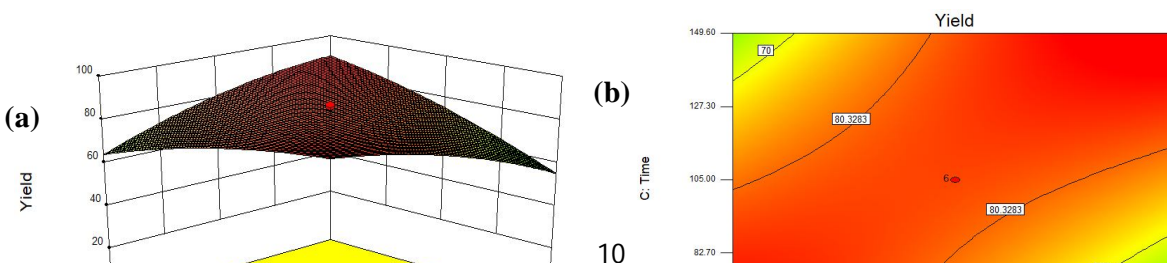
284 Since the “Lact-of-Fit F-value” is 2.52, thus means that there is a 16.62% chance that the model
 285 would not fit the experiment thereby proving the suitability of quadratic model for the experimental
 286 design.

287 The value of the coefficient of determination, often known as R², is a statistical metric that indicates
 288 the fraction of a dependent variable's variance that can be attributed to an independent variable or
 289 variables. The R² value provides a measure of how variability in the observed response values could
 290 be explained by the experimental factors and their interactions [63]. The R-squared (R²) value was
 291 0.9766 for methyl-ester (biodiesel) yield. The closer the R² value to 1, stronger the model and better it
 292 predicts the response. Therefore the R² value of 0.9766 showed that only about 2.34% of the total
 293 variation in the observed response cannot be explained by this model. In addition, the regression
 294 coefficient (R²) value of the actual experimental data (95%) and the predicted data (84.68%) result are
 295 obviously in resonance seeing that both values only differ by less than 11% and the coefficient of
 296 variance (error percentage) i.e. CV = 6.20% further proves that the model is a good fit. Similarly, the
 297 adequate precision of the model bothers around 21 which is largely greater than “4” (the minimum
 298 limit) because a signal to noise ratio of greater than 4 is desirable to indicate that the model is suitable
 299 for navigating the design space.

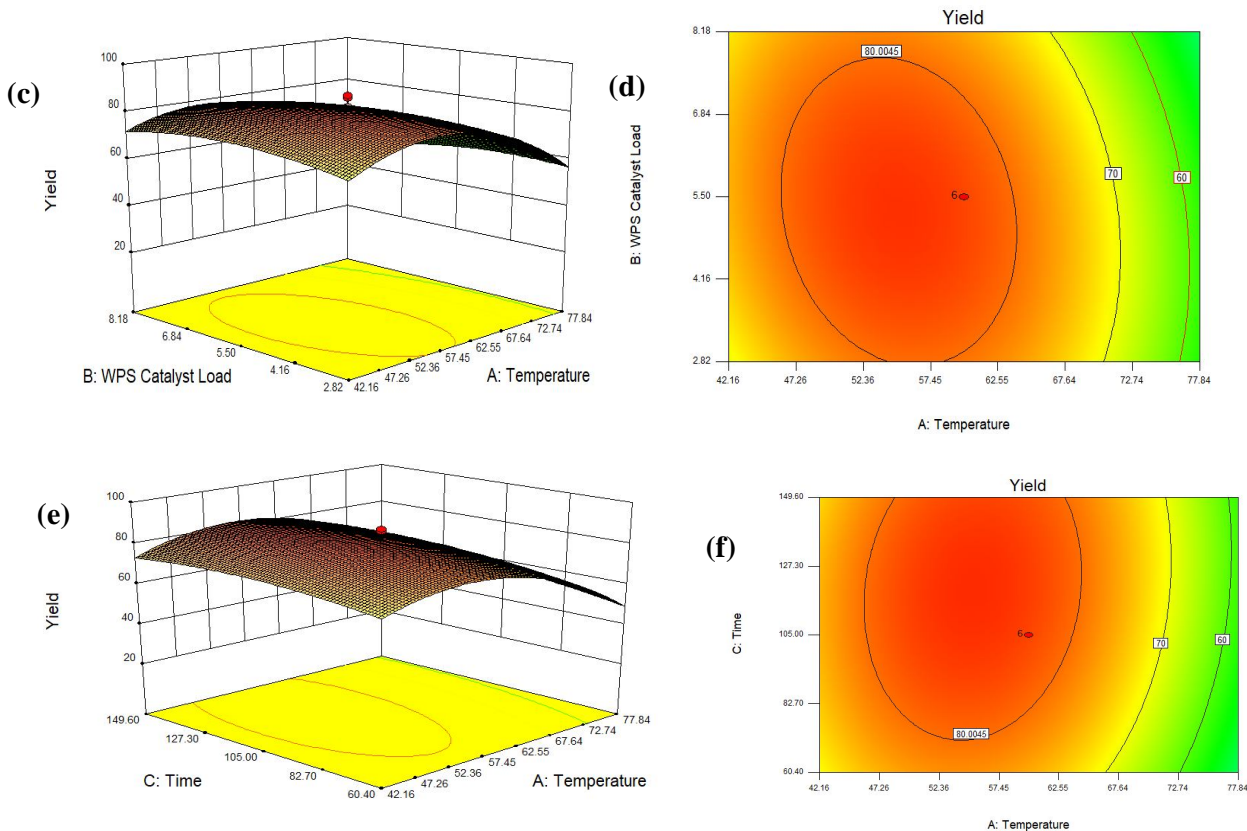


300 **Figure 4** Parity plot of Biodiesel yield produced via WFTS catalysts
 301

302 The consistency plotting (Figure 4) above demonstrates a significant correlation between the actual
 303 and expected values of biodiesel production. The points concentrated around the diagonal line
 304 indicating a successful fit of the model with an insignificant residual value due to the low variance
 305 between the actual and forecast values. The impacts of interaction process variables on biodiesel
 306 yield were graphically explored using three-dimensional surface plots and two-dimensional contour
 307 plots. The biodiesel production is projected to grow at optimal values but decline if the values are



308 increased past the optimum [49]. Figure 4a and 4b shows the interaction of reaction time and
 309 catalyst loading on the
 310



311
 312

313
 314

315 **Figure 5(a – f)** 3-D Response Surface and contour plots for the interaction effects of process
 316 parameters

317

318 biodiesel yield. It can be seen that the yield of biodiesel increases with increase in reaction time
 319 towards 105 minutes up to 5.5 wt.% WTFS catalyst at a reaction temperature of 60 °C and after that,
 320 a steady fall in the yield with increase in the amount of WTFS catalyst and reaction time. The shape of
 321 contour plot revealed that more than 80% of biodiesel yield peaked between 2.82 and about 5.5 wt. %
 322 WTFS catalyst and 60 – 105 minutes' reaction time. However, there is a reduction in yield with longer
 323 time spent and larger amount of WTFS catalyst. This may be because of presence of excess catalyst
 324 which will in turn, make the separation of products very difficult by which the amount of catalyst must
 325 be optimized [64]. Adequate time is required for reactants to interact together to form product(s) [65].
 326 Based on the results, it can be deduced that the reaction time and WTFS catalyst load play an
 327 important role in the biodiesel yield. Figure 4c and 4d demonstrates the effects of varied reaction
 328 temperatures and amounts of additional WTFS catalyst on biodiesel yield while the reaction duration
 329 was held constant at 105 minutes. Increase in reaction temperature had a substantial effect on
 330 biodiesel yield under all conditions. With a minute change in biodiesel yield due to the catalyst load,
 331 biodiesel yield rose according to the reaction temperature. However, yield decreases significantly with
 332 increasing temperature and WTFS catalyst concentration. This may be due to the boiling point of
 333 methanol (65 °C), which renders it unavailable for reaction [66]. In contrast, raising the designated
 334 amount of catalyst had a modest effect on the biodiesel output at different reaction temperatures. The
 335 maximum biodiesel was produced by employing a WTFS catalyst of roughly 5.5% by weight and 60
 336 °C. Figure 4e and 4f illustrates the three-dimensional and contour response surface built to
 337 demonstrate the impact of the transesterification condition factors (temperature and reaction time) on
 338 biodiesel yield. The yield of biodiesel increases as the reaction temperature approaches 60 °C and
 339 the reaction time approaches 105 minutes with a WTFS catalyst loading of 5.5% by weight.

340 Approximately in the vicinity of the optimal time and temperature, the maximum yield was achieved.
 341 However, the reaction time has a more consistent effect on biodiesel yield than reaction temperature,
 342 as temperatures above 65 °C resulted in a significant decrease in biodiesel yield at various reaction
 343 durations. Based on the data, it might be concluded that the reaction temperature had a greater
 344 impact on the biodiesel yield than the reaction time.

345

346 **Table 6**

347 Quality of WCO, Biodiesel with EU and American Standards [67]–[71]

Property	WCO	Biodiesel (Prepared)	Biodiesel (EU & American Standards)	Petroleum Biodiesel
Relative density (15°C) kg/m ³	909.8	880	860 – 900	832.5
Kinematic Viscosity (at 40°C), mm ² /s	13.30	4.638	1.9 – 6.0	2.0 – 4.5
Acid value (mg KOH/g)	10.02	0.416	0.50 max	0.15
Peroxide value (meq/kg)	461.54	-	-	-
Iodine value (I ₂ /100g)	2167.87	92.57	120 max	-
Saponification value (mg KOH/g)	184.25	-	-	-
Ester value (mg KOH/g)	174.25	103.57	96.5 min	-
Free fatty acid content (%)	5.035	0.209	0.251 max	-
Percentage glycerol	9.53	-	0.240 max	-
Pour point (°C)	5.2	0.3	0	1
Flash point (°C)	156	104	120 – 130 min	55 min
Carbon-content (% m/m)	2.65	0.019	0.05 – 0.30 max	0.30 max
Cloud point (°C)	10	1.3	No Report	2
Calorific value (MJ/kg)	34.78	40.17	25.35 – 43.96	44 – 46

348

349 The density of the prepared biodiesel from WCO was found to be 5.30% higher than the average
 350 petrol diesel (0.8325 kg/m³) as seen in Table 6. This is confirmed because the (average) densities of
 351 over 30 investigated methyl esters from different bio-sources and over 18 works, ranged from 0.75 to
 352 0.904 kg/m³, with the overall average value being 0.8802 kg/m³ (i.e. almost 5% higher than the
 353 corresponding fossil diesel value) [18], [72]–[77]. Density can impact fuel consumption as fuel
 354 introduced into the combustion chamber is determined volumetrically [78]. Biodiesel fuels are, in
 355 general, characterized by higher density than conventional fossil diesel, which means that
 356 volumetrically operating fuel pumps will inject greater mass of biodiesel than fossil diesel fuel [79].
 357 Since the flow is controlled by volume, the expected peak power reduction for engines using B100 is
 358 only 5 to 7 % less than the fossil diesel because more (kg/m³) would flow and vaporize more
 359 efficiently given a set throttle (volume) [80]. It should be noted that biodiesel produces more than
 360 three times the energy as the same amount of fossil fuel. Biodiesel's higher Specific gravity and
 361 density relative to fossil diesel means that on road biodiesel blends are normally made by splash
 362 blending the biodiesel fuel on top of the conventional diesel fuel or fossil fuel [80].

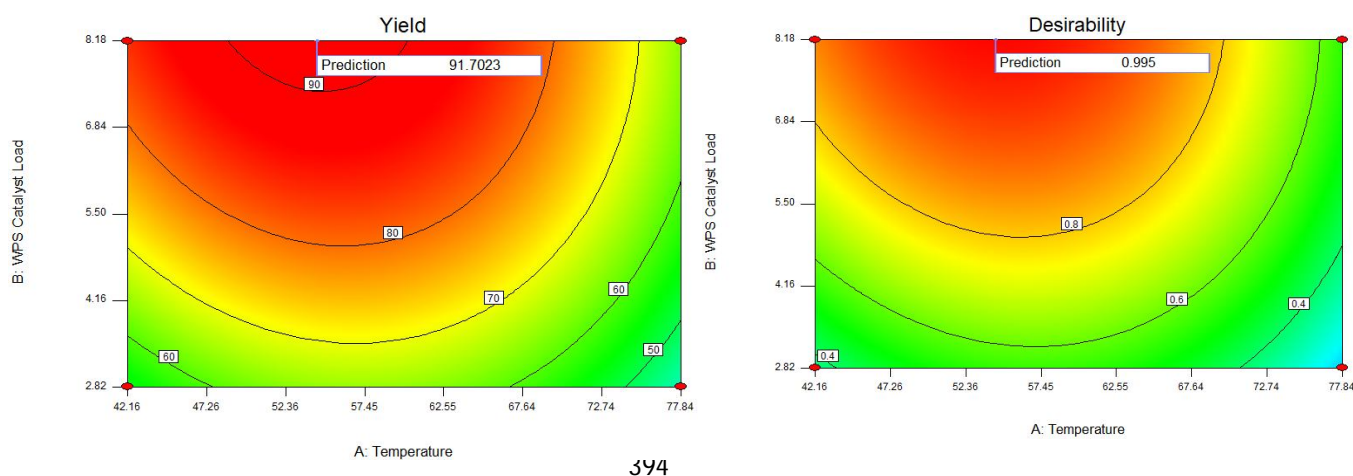
363 Kinematic viscosity is the primary reason why biodiesel is used as an alternative fuel instead of neat
 364 vegetable oils or animal fats [81]. The viscosity of the prepared biodiesel indicates a 65.187%
 365 decrease from the crude WCO. It is noticed that prepared biodiesel is 3.07% higher in value than the
 366 maximum allowable viscosity for a petroleum-derived diesel. The viscosity range given as per the
 367 ASTM D7042 and EN14214 standard is 1.9 to 6.0 mm²/s [67], [68]. This high value is due to high fatty
 368 acid composition of the source oil (WCO in this case) [82]. Fatty acid composition determines the
 369 degree of saturation and the higher the composition the higher the degree of saturation. Viscosity
 370 increases with increasing degree of saturation [69].

371 The produced biodiesel has a higher flash point than that of petroleum diesel (104 °C > 55 °C
 372 minimum) because biodiesel has a higher number of fatty acid methyl esters (FAME) which is
 373 generally not volatile. Flash point varies inversely with the fuel's volatility hence; biodiesel is safer to
 374 handle at higher temperature than fossil diesel. As diesel impurities increase in biodiesel and diesel-
 375 fuel blends, so does the flash point increase [78]. Flow properties such as pour point (PP) and cloud
 376 point (CP) are important in determining performance of fuel flow system [69]. Viscosity is known to be
 377 inversely proportional to temperature, therefore, operating a diesel engine at low temperatures
 378 especially in cold climate regions can be difficult because of high viscosities.

379 The acid value for the prepared biodiesel from WCO (0.416) was about 67% higher than petroleum
 380 diesel (0.15) but falls within the required American and European standard for biodiesel. However,
 381 this is an indication that the biodiesel is more unstable compared with petroleum diesel [69]. The
 382 calorific value increased by 15.5% from its source waste cooking oil but 13% lower than petroleum-
 383 diesel calorific values.

384 3.3.2 Optimization of biodiesel yield

385 Using the Design of Expert 8P software, biodiesel yield was numerically optimise by first optimizing all
 386 factors and response variables. Since maximum biodiesel yield is desired, set the lower (30.67%) and
 387 upper ranges (92 %). Table 4 codes independent variables as 1 and +1. Within the range, numerical
 388 optimization is performed. Based on the model and input criteria, the CCD provided the best system
 389 response optimizing biodiesel yield based on transesterification factors in experimental runs. The
 390 software projected that optimal parameters for biodiesel yield were 60 °C temperature, 5.5 wt. %
 391 WTFS catalyst load, and 105 minutes of reaction time, with 86.95 percent biodiesel yield. After
 392 optimization the biodiesel production was 91.7%. This signifies that the experimental value agreed
 393 with the model's value.



395 **Figure 6(a & b)** Contour plot of optimized biodiesel yield and desirability

396

397 4. CONCLUSION

398 The investigation on using waste *Typanotonus fuscatus* shell (WTFS) as a catalyst in
 399 transesterifying high FFA waste cooking oil (WCO) led to the following conclusions:

- 400 i. Waste cooking oil (WCO) had a large amount of free fatty acid (FFA > 5%), thus direct
 401 transesterification couldn't be done. Initial esterification decreased the FFA to 1%.
- 402 ii. Using design expert 8P's central composite design (CCD) of response surface methodology
 403 (RSM), the subsequent transesterification process successfully optimised biodiesel yield
 404 (91.7%). Experiment design favoured the quadratic model. **The three operating parameters
 405 were significant from the ANOVA results (< 0.05 p-values) showing that the prepared catalyst
 406 had an influence on the biodiesel yield. Only the interaction variable of catalyst load and time
 407 was significant while all quadratic variables showed significance.**
- 408 iii. The optimal reaction conditions were 60 °C, 5.5 wt. percent WTFS catalyst loading, and 105
 409 minutes at a 7:1 methanol-oil ratio. Biodiesel yields were 86.75 percent anticipated and 91.70
 410 percent optimised.
- 411 iv. X-ray diffraction and FTIR characterisation of WTFS showed the catalyst had a high
 412 percentage of CaO along with Al₂O₃, SiO₂, MgO, and traces of other metallic oxides,
 413 indicating WTFS is a promising catalyst source.
- 414 v. Gas chromatogram – mass spectroscopy (GCMS) analysis of improved biodiesel showed the
 415 presence of C16:0 (palmitic acid), C17:0 (methyl heptadecanoate), C18:1 (oleic acid), C18:2
 416 (linoleic acid), and C18:3 derivatives (linolenic acid). The physicochemical characterisation

417 indicated similar qualities to American and European biodiesel, making it appropriate for
418 blends and unblended application.

419 **Funding**

420 This work receives no fund from any University, Private organization or Government body.

421 **CRedit authorship contribution statement**

422 Ubani Oluwaseun Amune: Conceptualization, Methodology, Software, Validation, Formal analysis,
423 Investigation, Resources, Data curation, Writing both original draft and electronic draft.

424 Kevin Shegun Otoikhian: Formal analysis, Investigation, Resources, Data curation, Provide Financial
425 Support, Methodology, Software, Supervision

426 **Declaration of competing interest**

427 The authors declare that they have no known competing financial interests or personal relationships
428 that could have appeared to influence the work reported in this paper.

429 **References**

- 430 [1] J. Mercy Nisha Pauline, R. Sivaramakrishnan, A. Pugazhendhi, T. Anbarasan, and A. Achary,
431 'Transesterification kinetics of waste cooking oil and its diesel engine performance', *Fuel*, vol.
432 285, p. 119108, Feb. 2021, doi: 10.1016/j.fuel.2020.119108.
- 433 [2] A. S. Yusuff, A. O. Gbadamosi, and L. T. Popoola, 'Biodiesel production from transesterified
434 waste cooking oil by zinc-modified anthill catalyst: Parametric optimization and biodiesel
435 properties improvement', *Journal of Environmental Chemical Engineering*, vol. 9, no. 2, p.
436 104955, Apr. 2021, doi: 10.1016/j.jece.2020.104955.
- 437 [3] J. C. C. Santana *et al.*, 'Clean Production of Biofuel from Waste Cooking Oil to Reduce
438 Emissions, Fuel Cost, and Respiratory Disease Hospitalizations', *Sustainability*, vol. 13, no. 16,
439 p. 9185, Aug. 2021, doi: 10.3390/su13169185.
- 440 [4] M. Kuniyil *et al.*, 'Production of biodiesel from waste cooking oil using ZnCuO/N-doped
441 graphene nanocomposite as an efficient heterogeneous catalyst', *Arabian Journal of Chemistry*,
442 vol. 14, no. 3, p. 102982, Mar. 2021, doi: 10.1016/j.arabjc.2020.102982.
- 443 [5] N. S. Azman, T. S. Marliza, N. A. Mijan, T. Y. Y. Hin, and N. Khairuddin, 'Production of Biodiesel
444 from Waste Cooking Oil via Deoxygenation Using Ni-Mo/Ac Catalyst', p. 12, 2021.
- 445 [6] Y. S. Erchamo, 'Improved biodiesel production from waste cooking oil with mixed methanol-
446 ethanol using enhanced eggshell-derived CaO nano-catalyst', *Scientific Reports*, p. 12, 2021.
- 447 [7] F. Nadeem, 'Eco-benign biodiesel production from waste cooking oil using eggshell derived
448 MM-CaO catalyst and condition optimization using RSM approach', p. 11.
- 449 [8] S. Katekaew, 'Optimization of performance and exhaust emissions of single-cylinder diesel
450 engines fueled by blending diesel-like fuel from Yang-hard resin with waste cooking oil biodiesel
451 via response surface methodology', p. 12, 2021.
- 452 [9] Y. Liu, 'Economic evaluation and production process simulation of biodiesel production from
453 waste cooking oil', p. 55.
- 454 [10] M. M. Naeem, E. G. Al-Sakkari, D. C. Boffito, M. A. Gadalla, and F. H. Ashour, 'One-pot
455 conversion of highly acidic waste cooking oil into biodiesel over a novel bio-based bi-functional
456 catalyst', *Fuel*, vol. 283, p. 118914, Jan. 2021, doi: 10.1016/j.fuel.2020.118914.
- 457 [11] Y. H. Tan, M. O. Abdullah, C. Nolasco-Hipolito, and Y. H. Taufiq-Yap, 'Waste ostrich- and
458 chicken-eggshells as heterogeneous base catalyst for biodiesel production from used cooking
459 oil: Catalyst characterization and biodiesel yield performance', *Applied Energy*, vol. 160, pp. 58-
460 70, Dec. 2015, doi: 10.1016/j.apenergy.2015.09.023.
- 461 [12] S. Rezanía *et al.*, 'Review on transesterification of non-edible sources for biodiesel production
462 with a focus on economic aspects, fuel properties and by-product applications', *Energy
463 Conversion and Management*, vol. 201, p. 112155, Dec. 2019, doi:
464 10.1016/j.enconman.2019.112155.
- 465 [13] L. B. Moyo, S. E. Iyuke, R. F. Muvhiiwa, G. S. Simate, and N. Hlabangana, 'Application of
466 response surface methodology for optimization of biodiesel production parameters from waste
467 cooking oil using a membrane reactor', *South African Journal of Chemical Engineering*, vol. 35,
468 pp. 1-7, Jan. 2021, doi: 10.1016/j.sajce.2020.10.002.
- 469 [14] M. Arrais Gonçalves, E. Karine Lourenço Mares, J. Roberto Zamian, G. Narciso da Rocha Filho,
470 and L. Rafael Vieira da Conceição, 'Statistical optimization of biodiesel production from waste

- 471 cooking oil using magnetic acid heterogeneous catalyst MoO₃/SrFe₂O₄', *Fuel*, vol. 304, p.
 472 121463, Nov. 2021, doi: 10.1016/j.fuel.2021.121463.
- 473 [15] N. M. Maegala, S. Anupriya, A. Hazeeq Hazwan, Y. Nor Suhaila, and A. Hasdianty, 'Conversion
 474 of Waste Cooking Oil to Glycerol by Halal Microbial Lipase', *IOP Conf. Ser.: Earth Environ. Sci.*,
 475 vol. 505, no. 1, p. 012056, Jul. 2020, doi: 10.1088/1755-1315/505/1/012056.
- 476 [16] M. Loizides, X. Loizidou, D. Orthodoxou, and D. Petsa, 'Circular Bioeconomy in Action:
 477 Collection and Recycling of Domestic Used Cooking Oil through a Social, Reverse Logistics
 478 System', *Recycling*, vol. 4, no. 2, p. 16, Apr. 2019, doi: 10.3390/recycling4020016.
- 479 [17] S. K. Bhatia *et al.*, 'Conversion of waste cooking oil into biodiesel using heterogenous catalyst
 480 derived from cork biochar', *Bioresource Technology*, vol. 302, p. 122872, Apr. 2020, doi:
 481 10.1016/j.biortech.2020.122872.
- 482 [18] K. R. Bukkarapu, 'Comparative study of different biodiesel–diesel blends', *International Journal
 483 of Ambient Energy*, vol. 40, no. 3, pp. 295–303, Apr. 2019, doi:
 484 10.1080/01430750.2017.1393775.
- 485 [19] D. Singh-Ackbarali, R. Maharaj, N. Mohamed, and V. Ramjattan-Harry, 'Potential of used frying
 486 oil in paving material: solution to environmental pollution problem', *Environ Sci Pollut Res*, vol.
 487 24, no. 13, pp. 12220–12226, May 2017, doi: 10.1007/s11356-017-8793-z.
- 488 [20] M. E. Borges and L. Díaz, 'Recent developments on heterogeneous catalysts for biodiesel
 489 production by oil esterification and transesterification reactions: A review', *Renewable and
 490 Sustainable Energy Reviews*, vol. 16, no. 5, pp. 2839–2849, Jun. 2012, doi:
 491 10.1016/j.rser.2012.01.071.
- 492 [21] M. Helmi, 'Phosphomolybdic acid/graphene oxide as novel green catalyst using for biodiesel
 493 production from waste cooking oil via electrolysis method: Optimization using with response
 494 surface methodology (RSM)', p. 16.
- 495 [22] C. P. Okonkwo, V. I. E. Ajiwe, E. C. Mmaduakor, and N. V. Nwankwo, 'Modelling and
 496 Optimization of Biodiesel Production Process Parameters from Jansa Seed Oil (*Cussonia
 497 bateri*) Using Artificial Neural Network', *American Journal of Applied Chemistry*, p. 8.
- 498 [23] A. Gouran, 'Biodiesel production from waste cooking oil using wheat bran ash as a sustainable
 499 biomass', p. 9, 2021.
- 500 [24] M. Farooq, A. Ramli, and A. Naeem, 'Biodiesel production from low FFA waste cooking oil using
 501 heterogeneous catalyst derived from chicken bones', *Renewable Energy*, vol. 76, pp. 362–368,
 502 Apr. 2015, doi: 10.1016/j.renene.2014.11.042.
- 503 [25] M. Farooq *et al.*, 'Biodiesel production from date seed oil (*Phoenix dactylifera* L.) via egg shell
 504 derived heterogeneous catalyst', 2018, doi: 10.1016/J.CHERD.2018.02.002.
- 505 [26] C. E. Akhabue, E. O. Osa-Benedict, E. A. Oyedoh, and S. K. Otoikhian, 'Development of a bio-
 506 based bifunctional catalyst for simultaneous esterification and transesterification of neem seed
 507 oil: Modeling and optimization studies', *Renewable Energy*, vol. 152, pp. 724–735, Jun. 2020,
 508 doi: 10.1016/j.renene.2020.01.103.
- 509 [27] B. K. Uprety, W. Chaiwong, C. Ewelike, and S. K. Rakshit, 'Biodiesel production using
 510 heterogeneous catalysts including wood ash and the importance of enhancing byproduct
 511 glycerol purity', *Energy Conversion and Management*, vol. 115, pp. 191–199, May 2016, doi:
 512 10.1016/j.enconman.2016.02.032.
- 513 [28] F. Ezebor, M. Khairuddean, A. Z. Abdullah, and P. L. Boey, 'Oil palm trunk and sugarcane
 514 bagasse derived heterogeneous acid catalysts for production of fatty acid methyl esters',
 515 *Energy*, vol. 70, no. C, pp. 493–503, 2014.
- 516 [29] W. W. S. Ho, H. K. Ng, and S. Gan, 'Development and characterisation of novel heterogeneous
 517 palm oil mill boiler ash-based catalysts for biodiesel production', *Bioresource Technology*, vol.
 518 125, pp. 158–164, Dec. 2012, doi: 10.1016/j.biortech.2012.08.099.
- 519 [30] A. Endut *et al.*, 'Optimization of biodiesel production by solid acid catalyst derived from coconut
 520 shell via response surface methodology', *International Biodeterioration & Biodegradation*, vol.
 521 124, pp. 250–257, Oct. 2017, doi: 10.1016/j.ibiod.2017.06.008.
- 522 [31] A. O. Etim, E. Betiku, S. O. Ajala, P. J. Olaniyi, and T. V. Ojumu, 'Potential of Ripe Plantain Fruit
 523 Peels as an Ecofriendly Catalyst for Biodiesel Synthesis: Optimization by Artificial Neural
 524 Network Integrated with Genetic Algorithm', *Sustainability*, vol. 10, no. 3, Art. no. 3, Mar. 2018,
 525 doi: 10.3390/su10030707.
- 526 [32] M. Gohain, A. Devi, and D. Deka, 'Musa balbisiana Colla peel as highly effective renewable
 527 heterogeneous base catalyst for biodiesel production', *Industrial Crops and Products*, vol. 109,
 528 Aug. 2017, doi: 10.1016/j.indcrop.2017.08.006.
- 529 [33] J. Nisar *et al.*, 'Enhanced biodiesel production from *Jatropha* oil using calcined waste animal
 530 bones as catalyst', *Renewable Energy*, vol. 101, p. 111, Feb. 2017.

- 531 [34] S. V. Ranganathan, S. L. Narasimhan, and K. Muthukumar, 'An overview of enzymatic
532 production of biodiesel', *Bioresour Technol*, vol. 99, no. 10, pp. 3975–3981, Jul. 2008, doi:
533 10.1016/j.biortech.2007.04.060.
- 534 [35] P. E. Gama, R. A. da S. S. Gil, and E. R. Lachter, 'Produção de biodiesel através de
535 transesterificação in situ de sementes de girassol via catálise homogênea e heterogênea',
536 *Quím. Nova*, vol. 33, pp. 1859–1862, 2010, doi: 10.1590/S0100-40422010000900007.
- 537 [36] V. J. Aimikhe and G. B. Lekia, 'An Overview of the Applications of Periwinkle (*Tympanotonus*
538 *fuscatus*) Shells', *CJAST*, pp. 31–58, Aug. 2021, doi: 10.9734/cjast/2021/v40i1831442.
- 539 [37] K. Mo, U. J. Alengaram, M. Jumaat, S. C. Lee, W. I. Goh, and C. W. Yuen, 'Recycling of
540 seashell waste in concrete: A review', 2018, doi: 10.1016/J.CONBUILDMAT.2017.12.009.
- 541 [38] Y. Hou *et al.*, 'Marine shells: Potential opportunities for extraction of functional and health-
542 promoting materials', *Critical reviews in environmental science and technology*, 2016, Accessed:
543 May 30, 2022. [Online]. Available: <https://doi.org/10.1080/10643389.2016.1202669>
- 544 [39] A. Piker, B. Tabah, N. Perkas, and A. Gedanken, 'A green and low-cost room temperature
545 biodiesel production method from waste oil using egg shells as catalyst', *Fuel*, vol. 182, pp. 34–
546 41, Oct. 2016, doi: 10.1016/j.fuel.2016.05.078.
- 547 [40] N. Viriya-empikul, P. Krasae, B. Puttasawat, B. Yoosuk, N. Chollacoop, and K. Faungnawakij,
548 'Waste shells of mollusk and egg as biodiesel production catalysts', *Bioresource Technology*,
549 vol. 101, no. 10, pp. 3765–3767, May 2010, doi: 10.1016/j.biortech.2009.12.079.
- 550 [41] 'Waste shells of mollusk and egg as biodiesel production catalysts - ScienceDirect'.
551 <https://www.sciencedirect.com/science/article/abs/pii/S0960852409017441> (accessed May 30,
552 2022).
- 553 [42] E. Kurniawan and F. Perdana, 'BIODIESEL PRODUCTION OF WASTE COOKING OIL
554 CATALYZED BY CAO DERIVED FROM SNAIL (ACHATINA FULICA) SHELL WASTE', *Journal*
555 *of Chemical Process and Material Technology*, vol. 1, no. 1, Art. no. 1, Jan. 2022, doi:
556 10.36499/jcpmt.v1i1.5860.
- 557 [43] S. Phewphong, W. Roschat, P. Pholsupho, P. Moonsin, V. Promarak, and B. Yoosuk, 'Biodiesel
558 production process catalyzed by acid-treated golden apple snail shells (*Pomacea canaliculata*)-
559 derived CaO as a high-performance and green catalyst', *Eng Appl Sci Res*, vol. 49, no. 1, Art.
560 no. 1, 2022.
- 561 [44] S. Kaewdaeng, P. Sintuya, and R. Nirunsin, 'Biodiesel production using calcium oxide from river
562 snail shell ash as catalyst', *Energy Procedia*, vol. 138, pp. 937–942, Oct. 2017, doi:
563 10.1016/j.egypro.2017.10.057.
- 564 [45] H. Liu *et al.*, 'Mixed and ground KBr-impregnated calcined snail shell and kaolin as solid base
565 catalysts for biodiesel production', *Renewable Energy*, vol. 93, pp. 648–657, Aug. 2016, doi:
566 10.1016/j.renene.2016.03.017.
- 567 [46] A. D. Ogunsola, M. O. Durowoju, A. O. Alade, S. O. Jekayinfa, and O. Ogunkunle, 'Modeling
568 and optimization of two-step shea butter oil biodiesel synthesis using snail shells as
569 heterogeneous base catalysts', *Energy Advances*, vol. 1, no. 2, pp. 113–128, 2022, doi:
570 10.1039/D1YA00042J.
- 571 [47] 'Optimization and kinetic study of biodiesel production from *Hydnocarpus wightiana* oil and dairy
572 waste scum using snail shell CaO nano catalyst - ScienceDirect'.
573 <https://www.sciencedirect.com/science/article/abs/pii/S0960148119310018> (accessed May 30,
574 2022).
- 575 [48] I. B. Laskar, K. Rajkumari, R. Gupta, S. Chatterjee, B. Paul, and S. L. Rokhum, 'Waste snail
576 shell derived heterogeneous catalyst for biodiesel production by the transesterification of
577 soybean oil', *RSC Adv.*, vol. 8, no. 36, pp. 20131–20142, 2018, doi: 10.1039/C8RA02397B.
- 578 [49] A. S. Silitonga *et al.*, 'Biodiesel synthesis from *Ceiba pentandra* oil by microwave irradiation-
579 assisted transesterification: ELM modeling and optimization', *Renewable Energy*, vol. 146, pp.
580 1278–1291, Feb. 2020, doi: 10.1016/j.renene.2019.07.065.
- 581 [50] T. F. Adepoju, M. A. Ibeh, E. N. Udoetuk, and E. O. Babatunde, 'Quaternary blend of *Carica*
582 *papaya* - *Citrus sinensis* - *Hibiscus sabdariffa* - Waste used oil for biodiesel synthesis using CaO-
583 based catalyst derived from binary mix of *Lattorina littorea* and *Macra coralline* shell',
584 *Renewable Energy*, vol. 171, pp. 22–33, Jun. 2021, doi: 10.1016/j.renene.2021.02.020.
- 585 [51] J. G. Akpa and K. K. Dagde, 'Effect of Activation Method and Agent on the Characterization of
586 Prewinkle Shell Activated Carbon', *Chemical and Process Engineering Research*, vol. 56, no. 0,
587 p. 24, 2018.
- 588 [52] U. D. Offiong and G. E. Akpan, 'Assessment of Physico-Chemical Properties of Periwinkle Shell
589 Ash as Partial Replacement for Cement in Concrete', vol. 1, no. 7, p. 4, 2017.

- 590 [53] N. A. S. Amin, W. N. N. Omar, N. Nordin, and M. Mohamed, 'A Two-Step Biodiesel Production
591 from Waste Cooking Oil: Optimization of Pre-Treatment Step', *Journal of Applied Sciences*, vol.
592 9, no. 17, pp. 3098–3103, Dec. 2009, doi: 10.3923/jas.2009.3098.3103.
- 593 [54] H. Sanli and M. Canakci, 'Effects of Different Alcohol and Catalyst Usage on Biodiesel
594 Production from Different Vegetable Oils', *Energy Fuels*, vol. 22, no. 4, pp. 2713–2719, Jul.
595 2008, doi: 10.1021/ef700720w.
- 596 [55] B. Thangaraj, P. R. Solomon, B. Muniyandi, S. Ranganathan, and L. Lin, 'Catalysis in biodiesel
597 production—a review', *Clean Energy*, vol. 3, no. 1, pp. 2–23, Feb. 2019, doi: 10.1093/ce/zky020.
- 598 [56] S. Yan, M. Kim, S. Salley, and K. Ng, 'Oil transesterification over calcium oxides modified with
599 lanthanum', 2009, doi: 10.1016/J.APCATA.2009.03.015.
- 600 [57] M. Keihani, H. Esmaili, and P. Rouhi, 'Biodiesel Production from Chicken Fat Using Nano-
601 calcium Oxide Catalyst and Improving the Fuel Properties via Blending with Diesel', *PCR*, vol. 6,
602 no. 3, Sep. 2018, doi: 10.22036/pcr.2018.114565.1453.
- 603 [58] T. Eryilmaz, 'Process optimization for biodiesel production from neutralized waste cooking oil
604 and the effect of this biodiesel on engine performance', *CT&F Cienc. Tecnol. Futuro*, vol. 8, no.
605 1, pp. 121–127, Jun. 2018, doi: 10.29047/01225383.99.
- 606 [59] H. Musa, D. Eric, A. Hassan, B. Usman, N. F. Isa, and A. S. Alhassan, 'Optimized Biodiesel
607 Production from *jatropha curcas* oil', *Energy Research Journal*, vol. 12, no. 1, pp. 39–44, Jan.
608 2021, doi: 10.3844/erjsp.2021.39.44.
- 609 [60] A. Fatima, M. Zafar, M. Ahmad, S. Sultana, and M. I. Ali, 'Parametric characterization and
610 statistical optimization of Argemone ochroleuca (Mexican Poppy) methyl esters as a renewable
611 source of energy', *null*, vol. 39, no. 19, pp. 1963–1969, Oct. 2017, doi:
612 10.1080/15567036.2017.1391896.
- 613 [61] D. Leung and Y. Guo, 'Transesterification of neat and used frying oil: Optimization for biodiesel
614 production', *Fuel Processing Technology*, vol. 87, pp. 883–890, Oct. 2006, doi:
615 10.1016/j.fuproc.2006.06.003.
- 616 [62] T. F. Adepoju, 'Optimization processes of biodiesel production from pig and neem (*Azadirachta*
617 *indica* a.Juss) seeds blend oil using alternative catalysts from waste biomass', *Industrial Crops*
618 *and Products*, vol. 149, p. 112334, Jul. 2020, doi: 10.1016/j.indcrop.2020.112334.
- 619 [63] Y. Tang, G. Chen, J. Zhang, and Y. Lu, 'Highly active CaO for the transesterification to biodiesel
620 production from rapeseed oil', 1, vol. 25, no. 1, Art. no. 1, 2011, doi: 10.4314/bcse.v25i1.63359.
- 621 [64] F. Trejo-Zárraga, F. de J. Hernández-Loyo, J. C. Chavarría-Hernández, and R. Sotelo-Boyás,
622 *Kinetics of Transesterification Processes for Biodiesel Production*. IntechOpen, 2018. doi:
623 10.5772/intechopen.75927.
- 624 [65] B. O. Ighose, I. A. Adeleke, M. Damos, H. A. Junaid, K. E. Okpalaeke, and E. Betiku,
625 'Optimization of biodiesel production from *Thevetia peruviana* seed oil by adaptive neuro-fuzzy
626 inference system coupled with genetic algorithm and response surface methodology', 2017,
627 Accessed: Jun. 06, 2022. [Online]. Available: <https://pubag.nal.usda.gov/catalog/6101872>
- 628 [66] M. Mansourpoor, 'Optimization of Biodiesel Production from Sunflower Oil Using Response
629 Surface Methodology', *Journal of Chemical Engineering & Process Technology*, vol. 03, Jan.
630 2012, doi: 10.4172/2157-7048.1000141.
- 631 [67] I. Barabas and I.-A. Todoru, 'Biodiesel Quality, Standards and Properties', in *Biodiesel- Quality,*
632 *Emissions and By-Products*, G. Montero, Ed. InTech, 2011. doi: 10.5772/25370.
- 633 [68] G. Montero and M. Stoytcheva, *Biodiesel-Quality, Emissions and By-Products*. 2011.
- 634 [69] G. K. Ayetor, A. Sunnu, and J. Parbey, 'Effect of biodiesel production parameters on viscosity
635 and yield of methyl esters: *Jatropha curcas*, *Elaeis guineensis* and *Cocos nucifera*', *Alexandria*
636 *Engineering Journal*, vol. 54, no. 4, pp. 1285–1290, Dec. 2015, doi: 10.1016/j.aej.2015.09.011.
- 637 [70] 'EN 14214', *Wikipedia*. Nov. 07, 2021. Accessed: Jun. 04, 2022. [Online]. Available:
638 https://en.wikipedia.org/w/index.php?title=EN_14214&oldid=1054080525
- 639 [71] 'Alternative Fuels Data Center: ASTM Biodiesel Specifications'.
640 https://afdc.energy.gov/fuels/biodiesel_specifications.html (accessed Jun. 04, 2022).
- 641 [72] L. F. Ramírez Verduzco, 'Density and viscosity of biodiesel as a function of temperature:
642 Empirical models', *Renewable and Sustainable Energy Reviews*, vol. 19, pp. 652–665, Mar.
643 2013, doi: 10.1016/j.rser.2012.11.022.
- 644 [73] M. J. Pratas, S. Freitas, M. B. Oliveira, S. C. Monteiro, Á. S. Lima, and J. A. P. Coutinho,
645 'Densities and Viscosities of Minority Fatty Acid Methyl and Ethyl Esters Present in Biodiesel', *J.*
646 *Chem. Eng. Data*, vol. 56, no. 5, pp. 2175–2180, May 2011, doi: 10.1021/je1012235.
- 647 [74] E. G. Giakoumis and C. K. Sarakatsanis, 'Estimation of biodiesel cetane number, density,
648 kinematic viscosity and heating values from its fatty acid weight composition', *Fuel*, vol. 222, pp.
649 574–585, Jun. 2018, doi: 10.1016/j.fuel.2018.02.187.

- 650 [75] K. Bencheikh *et al.*, 'Fuels properties, characterizations and engine and emission performance
651 analyses of ternary waste cooking oil biodiesel–diesel–propanol blends', *Sustainable Energy*
652 *Technologies and Assessments*, vol. 35, pp. 321–334, Oct. 2019, doi:
653 10.1016/j.seta.2019.08.007.
- 654 [76] M. Gülüm and A. Bilgin, 'A comprehensive study on measurement and prediction of viscosity of
655 biodiesel-diesel-alcohol ternary blends', *Energy*, vol. 148, pp. 341–361, Apr. 2018, doi:
656 10.1016/j.energy.2018.01.123.
- 657 [77] L. Razzaq *et al.*, 'Modeling Viscosity and Density of Ethanol-Diesel-Biodiesel Ternary Blends for
658 Sustainable Environment', *Sustainability*, vol. 12, no. 12, p. 5186, Jun. 2020, doi:
659 10.3390/su12125186.
- 660 [78] A. K. Hossain and P. A. Davies, 'Plant oils as fuels for compression ignition engines: A technical
661 review and life-cycle analysis', *Renewable Energy*, vol. 35, no. 1, pp. 1–13, 2010.
- 662 [79] B. Tesfa, R. Mishra, F. Gu, and N. Powles, 'Prediction models for density and viscosity of
663 biodiesel and their effects on fuel supply system in CI engines', *Renewable Energy*, vol. 35, no.
664 12, pp. 2752–2760, Dec. 2010, doi: 10.1016/j.renene.2010.04.026.
- 665 [80] Md. N. Nabi, Md. M. Rahman, and Md. S. Akhter, 'Biodiesel from cotton seed oil and its effect
666 on engine performance and exhaust emissions', *Applied Thermal Engineering*, vol. 29, no. 11,
667 pp. 2265–2270, Aug. 2009, doi: 10.1016/j.applthermaleng.2008.11.009.
- 668 [81] B. Moser, 'Biodiesel Production, Properties, and Feedstocks', in *In Vitro Cellular &*
669 *Developmental Biology - Plant*, vol. 45, 2010, pp. 285–347. doi: 10.1007/978-1-4419-7145-
670 6_15.
- 671 [82] M. M. Roy, W. Wang, and J. Bujold, 'Biodiesel production and comparison of emissions of a DI
672 diesel engine fueled by biodiesel–diesel and canola oil–diesel blends at high idling operations',
673 *Applied Energy*, vol. 106, no. C, pp. 198–208, 2013.
- 674